Excitation Transfer in Aggregated and Linearly Confined Poly(*p*-phenylene vinylene) Chains†

Gil C. Claudio and Eric R. Bittner*

Department of Chemistry, University of Houston, Houston, Texas 77204

Received: December 17, 2002; In Final Form: February 11, 2003

We simulate the nonradiative excitation energy transfer in an ensemble of poly(*p*-phenylene vinylene) (PPV) chains the configurations of which were calculated using a random growth algorithm. The polymers are viewed as a series of phenyl−vinyl oligomers of various lengths, separated from one another through conformational defects. Initially excited chromophores, corresponding to short segments of PPV oligomers in the polymer, transfer excitations nonradiatively to longer oligomers of lower electronic energy with transfer rates as described by Förster theory. Transfer occurs in a short period of time (<50 ps) and within a small local area (∼52 Å) around the initially excited chromophore. We find in our simulations that the majority of the excitation gets trapped in local minima corresponding to medium length oligomers (with six to eight phenyl rings) and does not eventually find the global energy minimum. Excitation transfer dynamics are presented for PPV chains inserted into mesoporous silica matrixes, which are believed to direct the excitation energy from the parts of the chains outside the pores to those inside the pores. We show that this funneling is most efficient if the chains outside the pores are close enough to the target chromophores inside the pores, within a distance defined by an average transfer correlation length.

I. Introduction

One of the most interesting class of materials being developed for light-emitting devices (LEDs) is organic-based. The main feature of these organic molecules, whether monomeric or polymeric, is the presence of an extended π-conjugation. The primary excitations are predominantly associated with the π electron structure, the main spectral features arising from $\pi-\pi^*$ transitions. Though the light-emitting process can be explained simply as a vertical relaxation to the ground state, many spectral data have shown a number of possible processes that can occur between excitation and emission thus complicating the actual explanation of the process of emission. These processes usually involve migration of the excited species to the lowest-energy state. Thus, as Kasha's rule states,[1] the radiative transition to the ground state in a given spin manifold originates from the lowest excited state. Energy migration from one chromophore to another can include nonradiative excitation transfer, which can occur between the femtosecond and tens of a picosecond range, and migration of bound electron−hole pairs, which usually occur at a slower rate in the range of hundreds of a picosecond. However, in most systems, the slowest of these migration processes is still at least 1 order of magnitude faster than the natural radiative lifetime of a chromophore. All of these competing migration processes therefore have a profound effect even in a simple steady-state emission spectrum of these organic LED materials.

In the case of poly(*p*-phenylene vinylene) (PPV) (trimer shown in Figure 1) and its soluble derivative MEH−PPV, nonradiative excitation transfer has been cited as one important process to interpret experimental results. Barbara et al.[2−4] indicated that efficient radiationless electronic energy transfer along the chain occurs prior to oxygen quenching to explain the discrete intensity levels in their time-dependent fluorescence of single-molecule spectroscopy of MEH−PPV. Schwartz and co-workers[5,6] have also shown radiationless excitation migration to be the main factor in their spectra of bulk MEH−PPV using different spectroscopic methods.

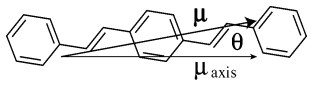

Figure 1. Transition dipole moment μ of PPV trimer (OPV3). A θ-value of 15° was used in this study.

In a conjugated polymer such as PPV, it is energetically favorable for the dihedral angle between phenyl and vinyl groups to be close to 0° to maximize conjugation. However, in the entire polymer, it is statistically probable for some of these angles to flip and thus break the conjugation.[7] The dihedral angle does not have to turn all the way to $\pi/2$ to break conjugation. In fact, Brédas et al.[8] suggested a dihedral angle of 40° as an acceptable cutoff for conjugation breaks. Instead of being an infinitely long conjugated system, PPV therefore can be regarded as a chain of conjugated phenyl−vinyl (Ph−V) oligomers of various lengths that act as both donor and acceptor chromophores in nonradiative excitation transfer. The energy band gaps of these oligomers are inversely proportional to the oligomer length ($E \propto 1/n$). The nonradiative excitation transfer starts from an initially excited high-energy short oligomer and transfers to lower-energy oligomers with longer oligomer lengths, until the lowest-energy oligomer emits a red-shifted photon.

The majority of the spectroscopic studies of PPV and its derivatives involve the coiled chain in many different environments, either in solution[9,10] or in a solid matrix,[2−4,9,10] all of which invoke nonradiative excitation transfer to explain their results. Aside from using these bulk PPV samples, a novel system was synthesized by Schwartz and co-workers[9,10] that

† Part of the special issue "Donald J. Kouri Festschrift".

10.1021/jp027746z CCC: $25.00
Published on Web 04/08/2003

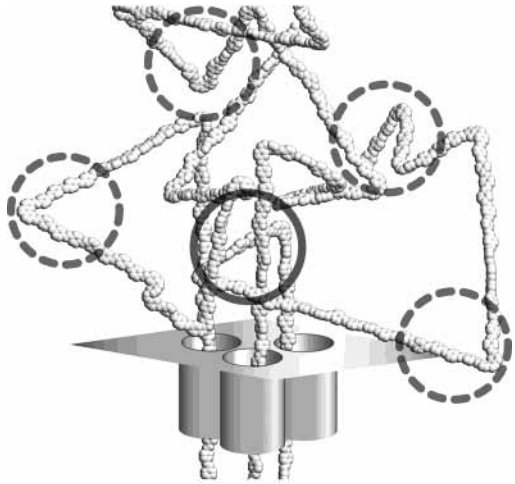

Figure 2. Calculated model of MEH−PPV embedded into channels of oriented, hexagonal mesoporous silica glass synthesized by Schwartz and et al.[9,10] Energy migrates from high-energy randomly oriented short oligomers outside the channels into the low-energy long oligomers that are aligned inside the channels. This system allows the energy to be directed into a specific region. In calculating the anisotropy of the model, we find that most of the excitation stays outside the channels (dashed circles) and only a few are able to migrate into the channels (solid circle).

involved chains of MEH−PPV embedded into channels of oriented, hexagonal mesoporous silica glass as shown schematically in Figure 2. One expects that the polymer outside the channel is composed of short randomly oriented oligomers that have a high excitation energy. On the other hand, the inside segments oriented along the direction of the porous glass must be composed of longer oligomer segments that have a lower excitation energy. Excitation energy migration is expected to proceed from the randomly oriented oligomers outside the channels into the lower-energy oligomer segments inside the channels. This system allows the energy to be directed into a specific region and serves as a model of light-harvesting systems.

In this paper, we simulate the nonradiative excitation transfer in PPV with a point-dipole approximation. First, a brief summary of Förster theory is presented explaining the nature and mechanics of nonradiative excitation transfer. This energy-transfer process is then calculated in single chains of PPV. The method of obtaining the parameters needed for this calculation has been reported[7,11] and is summarized in the next section. This section also includes a brief description of the polymer−mesoporous silica experiments of Schwartz and co-workers[9,10] and our simulations to model their experiments. We end the methodology section by discussing time-dependent fluorescence anisotropy, which can measure the extent of energy transfer. The next section presents and discusses the results of our calculations, and in the last section, we present our conclusions.

II. Methodology

A. Nonradiative Energy Transfer. Nonradiative excitation transfer from a donor chromophore to an acceptor can be mediated through dipole−dipole interaction. This process, although intrinsically radiationless, can be formally viewed as the combined donor emission and simultaneous acceptor absorption. In the strong coupling limit or the coherent transfer case, excitation energy transfer is faster than intermolecular and intramolecular relaxation of both donor and acceptor. On the other hand, if energy transfer is strongly affected by the vibrational relaxations of the system, coupling is weak and transfer is incoherent, in which case a simple two-level system approximation used in coherent states is not valid. This assumes that the densities of vibrational states of both donor and acceptor are important in incoherent transfer. And because the vibrational relaxation is mainly due to the intrinsic characteristics of the chromophore and not to coupling with its surrounding, this weak coupling limit occurs in systems with homogeneously broadened spectra. Förster's[12] theory for the rate of incoherent transfer between two chromophores gives a set of equations describing this process. It is strictly valid only for homogeneously broadened spectra.[13] Semiempirical calculations by Karabunarliev et al.[14] suggest this to be true for the case for PPV and its oligomers.

The strong influence of the vibrational relaxation of the system implies that upon photoexcitation, a chromophore rapidly and irreversibly disperses the excess electron energy to its vibrational states. This red-shifted state acts as the excitation donor to other chromophores resulting in a red-shifted emission spectrum. In terms of OPVs, an oligomer can act as a donor only to other oligomers with the same or lower energy than itself, that is, oligomers of the same or greater number of phenyl rings.

Förster's theory is a point-dipole approximation, in which the only spatial parameters are the relative orientation of the chromophores and the distance between their midpoints. A more detailed calculation of the transfer rate is the distributed monopole method,[15] where the total coupling between the two chromophores is estimated as the sum over atomic transition charges and is therefore more sensitive to the particular shapes of both donor and acceptor. The difference between the two methods will be discussed in another paper.[16] The rate of Förster transfer from chromophore *i* (donor) to *j* (acceptor) is given by the equation[17]

$$k_{ji} = \frac{3}{2}\kappa^2 \frac{1}{\tau_0}\left(\frac{R_0}{r_{ij}}\right)^6 \tag{1}$$

The distance between the donor and the acceptor is r_{ij}. τ_0 is the natural lifetime (spontaneous emission rate) of the donor and can be calculated using

$$\frac{1}{\tau_0} = \frac{\omega^3 e^2}{3\hbar c^3 \pi \epsilon_0} |\langle x \rangle|^2 \tag{2}$$

where $\langle x \rangle$ is the transition dipole moment of the chromophore calculated for vertical S_0 to S_1 transitions obtained by the AM1-CI model.[18] From this equation, we can conclude that the radiative lifetime of the different oligomers decreases with increasing oligomer size[1] because the dipole factor is directly proportional to the oligomer size. κ^2 is the dipole coupling orientation factor, which is given by

$$\kappa^2 = [\mathbf{r}_i \cdot \mathbf{r}_j - 3(\mathbf{R} \cdot \mathbf{r}_i)(\mathbf{R} \cdot \mathbf{r}_j)]^2 \tag{3}$$

where $\mathbf{r}_i$ ($\mathbf{r}_j$) is the unit vector of the donor (acceptor) and $\mathbf{R}$ is the unit vector between the midpoints of the donor and acceptor. The average of this factor for a set of randomly oriented chromophores is $^2/_3$. In this study, the value of this factor is explicitly calculated for every combination of donor and acceptor chromophores in an ensemble of PPV chains.

The Förster distance, R_0, is the distance at which the rate of transfer from the donor to the acceptor is equal to the decay rate of the donor in the absence of acceptors. The Förster distance is proportional to the amount of overlap between the

donor emission spectrum and the acceptor absorption spectrum. It can be expanded in various forms, one of which being

$$R_0^6 = 5.86 \times 10^{-25} \frac{\eta_0}{n^4} \int_0^\infty F(\bar{\nu}) \epsilon(\bar{\nu}) \frac{d\bar{\nu}}{\bar{\nu}^4} \quad (4)$$

η_0 is the quantum yield of the donor luminescence, taken as 0.27,[1,19] and n is the refractive index of the solvent, taken as unity. $F(\bar{\nu})$ is the normalized emission spectrum of the donor, and $\epsilon(\bar{\nu})$ is the molar extinction coefficient of the acceptor. In this study, we use $\epsilon_{max} = 10^4\ M^{-1}\ cm^{-1}$, which is in the range of spin- and orbitally allowed transitions ($10^3 \le \epsilon_{max} \le 10^5$).[20] For comparison, we also calculated the excitation transfer using the end points of this extinction coefficient range. We are not aware of any study that reports the exact molar extinction coefficient for PPV or any of its oligomers. One might think that a random choice of a parameter value within a range of 2 orders of magnitude may be totally arbitrary. Indeed, as will be shown in the results, the exact extent of excitation transfer is highly dependent on the parameters for the calculations. However, it will also be shown that an estimate of this parameter is sufficient to elucidate the essential properties of excitation transfer.

The chromophores in PPV chains are the PV oligomers (OPV) of various lengths, which are separated by conjugation breaks within the chain, and different R_0 values can be derived for every combination of donor and acceptor oligomer lengths allowing us to generate a catalog of Förster radii between different chromophore pairs. However, to achieve spectral overlap and Förster transfer, the acceptor should at least be of the same oligomer length as the donor. We assume that at $T =$ 300 K reverse energy transfer does not occur when the acceptor is shorter than the donor, in which case the R_0 values are equal to 0.

Brédas and co-workers[21,22] characterized the absorption and emission spectra of PV oligomers containing from two to five phenyl rings. The total absorption (emission) spectrum can be written as a sum of the spectra from the lowest vibrational state of the chromophore in the ground (excited) state to the various vibrational levels of the excited (ground) state. The relative intensities of these transitions are given by a Poisson distribution. The functional form of both absorption and emission (A/E) spectra is given by

$$f_{A/E}(\bar{\nu}) = \sum_{n=0}^{\infty} \frac{\exp^{-S} S^n}{n!} \frac{\Gamma}{(E_{A/E} \pm n\hbar\omega - \bar{\nu})^2 + \Gamma^2} \quad (5)$$

where $\hbar\omega$ is the vibronic energy level difference (0.15 eV, (+) for absorption and (−) for emission) and Γ is the spectral broadening. $E_{A/E}$ is the transition energy for absorption/emission, which is inversely proportional to the length of the oligomer ($E \propto 1/n$). ν is the vibrational level in the excited (ground) state, and S is the Huang−Rhys factor, which governs the relative intensities of the vibronic features in the absorption (emission) spectra. The values of Γ and $E_{A/E}$ for oligomers containing two to five phenyl rings were taken from Brédas and co-workers,[21,22] while those for longer oligomers were extrapolated from these values.

B. Intrachain Transport. Incoherent through-space Förster transfer can be very fast, depending on the distances between chromophores. An interchromophore distance that is half the Förster radius can have a transfer rate 2 orders of magnitude greater than the natural lifetime of the donor, which is on the order of less than 10 ps. In the case of two chromophores connected by one single bond but separated by a dihedral angle close to 90°, other through-bond excitation transfer mechanisms aside from Förster transfer can occur. As far as we know, only Schwartz[10] has reported an estimated rate of through-bond transfer at ~250 ps. This transfer occurs when the dihedral angle between previously unconjugated adjacent phenyl and vinyl groups turns to achieve conjugation. Such motions in the polymer case are relatively slow because the twists and turns of one group involves pulling the rest of the chain attached to it.

We propose a simple model that can relate the rate of excitation transfer between two chemically connected chromophores to the dihedral angle. The equation for the model is

$$\omega(\theta_{ij}) = \frac{1}{250\ ps}(2.5 \cos^2 \theta_{ij} + 0.1), \quad i = j \pm 1, \quad 40° < \theta_{ij} < 140° \quad (6)$$

The rate of $4 \times 10^{-3}\ ps^{-1}$ is tuned by a simple switching factor (expression inside the parenthesis), which is a function of the dihedral angle, θ_{ij}. The limits of the switching factor are 1.57 for 40° and 0.1 for 90°. The closer the angle is to the 40° cutoff,[8] the faster it can turn and establish conjugation between the two chromophores as represented by increase of the average rate by a factor of 1.57. Phenyl or vinyl groups separated from an adjacent oligomer by a dihedral angle of 90° need more time to switch back to an angle close to 0° and achive π-overlap, as represented by decrease of the average rate by a factor of 0.1. This switching factor has the same functional form as the one computed by Grozema et al.,[23] who studied the effect of torsional disorder in charge transfer between two conjugated units the configuration of which is separated by a torsion around the σ-bond. For comparison, we also calculated the excitation transfer neglecting this intrachain transport model.

C. Polymer Configuration. The equations that describe the nonradiative excitation transfer due to dipole−dipole coupling are highly dependent on the configuration of the system. The rate of transfer is dependent on the distance and the relative orientation between the two interacting chromophores. The Förster distances, R_0, are dependent on the oligomer lengths of the donors and acceptors, which are also determined by the configuration of the system. Though general distributions can be assigned to these variables, a more precise parametrization of polymer configuration can help us better understand the details of the migration. This necessitates the use of actual configurations of polymers.

We[7] calculated the energy accessible configurations of PPV using a random growth algorithm, which assumes that the configuration of a part of a polymer (a few monomers length) can be sampled from the configuration of an OPV trimer. The configuration of the trimer was taken as a Boltzmann-weighted probability calculated from the energy surface of the trimer.[11] The results of these studies showed that the oligomer (conjugation) length distributions are not Gaussian[24,25] but exhibit an exponential distribution, which is more consistent with experiment.[26,27] Several (11) polymer samples with 1000 Ph−V repeat units with an average of 10% cis-defect density were calculated using this algorithm. Each chain was separated into different oligomer units, each unit being a group of consecutive phenyl and vinyl groups that are conjugated to each other and are demarked from neighboring conjugation segments by conjugation breaks defined by a dihedral angle of 40°, as suggested by Brédas et al.[8] to be an acceptable cutoff for conjugation breaks. The lengths of these oligomer units and their relative orientation and distances were calculated from each sample. These param-

TABLE 1: Förster Distances (Å) between Ph−V Oligomers

n_ϕ[a]	2	3	4	5	6	7	8	9	10	11	12	13	14	≥15
2	24.8													
3	34.7	27.9												
4	34.5	35.3	29.6											
5	33.7	37.6	34.0	30.8										
6	32.2	39.0	37.7	35.9	31.5									
7	31.4	39.4	39.4	38.1	34.7	32.1								
8	30.7	39.4	40.3	39.5	37.0	34.6	32.6							
9	30.2	39.4	40.8	40.5	38.4	36.5	34.6	33.0						
10	29.7	39.3	41.2	41.1	39.5	37.9	36.2	34.6	33.3					
11	39.4	39.2	41.5	41.6	40.2	38.9	37.4	36.0	34.7	33.5				
12	29.1	39.0	41.6	41.9	40.9	39.7	38.4	37.0	35.8	34.7	33.7			
13	28.9	38.9	41.7	42.1	41.4	40.3	39.2	37.9	36.7	35.7	34.8	33.9		
14	28.7	38.8	41.8	42.3	41.8	40.8	39.8	38.6	37.5	36.5	35.6	34.8	34.1	
≥15	28.5	38.6	41.8	42.4	42.1	41.2	40.3	39.2	38.1	37.2	36.3	35.6	34.9	34.2

[a] Number of phenyl rings in the oligomer.

eters in turn were used to calculate the different rates of excitation transfer between the chromophores in the polymer samples.

Using this same algorithm, we also calculated sample configurations of PPV in mesoporous silica similar to the experimental system described by Schwartz and co-workers[9,10] as shown in Figure 2. The mesoporous matrix was represented as cylindrical wells, one end of each well opening to a flat surface. Each sample system consisted of three wells, 12 Å in radius, the centers of each well being 34 Å apart and one PPV chain being inserted in each well. A short-range repulsive force between the polymers and the walls of the well and the flat surface was also included. Each polymer consisted of 100 Ph−V monomers with at least 50 monomers inside the well. Finally, an average of five cis defects were introduced in the parts of the chain outside the tube to allow the chain to turn and coil onto itself and entangle with the neighboring chains.

D. Model Parameters. Using eq 2, we calculated the values for the natural lifetime of the oligomers. These vary with chain length and range from 300 to 612 ps. This is in general agreement with the PPV photoluminescence lifetime of 320 ps as measured by Greenham et al.[19] The dipole moments were calculated using AM1 with configuration interaction (CI), which accurately predicts the spectra of oligomers.[14] The values for the 0−0 emission and absorption energies, the Huang−Rhys factors for OPVs with two to five phenyl rings, and the broadening factors Γ for both absorption and emission spectra were taken from Brédas and co-workers[21,22] The values for hexamers and longer oligomers were extrapolated from these values using the fact that the absorption and emission energies and the Huang−Rhys factors are inversely proportional to the number of phenyl rings.

Given the 0−0 emission and absorption energies and the Huang−Rhys and broadening factors, one can calculate the absorption and emission spectra of the different oligomers as described by eq 5. These in turn were used to calculate the Förster distances using eq 4. Depending on the oligomer lengths of the donor and acceptor, these distances ranged from 24.8 to 42.4 Å, the average being 36.7 Å. These are listed in Table 1. If we assume that the absorption and emission spectra of oligomers with 15 or more phenyl rings are practically equal, the Förster distances involving these chromophores are taken to be equal to those of OPV-15. Finally, because we assume that excitation transfer goes only from one oligomer to another of the same or greater number of phenyl rings, the Förster distance and hence the transfer rate for longer to shorter oligomers are equal to zero.

E. Dynamics of Excitation Transfer. We can assume that the excitation migration in this multichromophoric system can be described by the Pauli master equation,

$$\frac{dP_i}{dt} = \sum_j [\omega_{ij} P_j - \omega_{ji} P_i] \tag{7}$$

where ω_{ji} is the Förster excitation energy transfer rate between two chromophores as described in the previous section and $P_i(t)$ is the time-dependent probability of an excitation residing in chromophore i. In molecular systems in which the dipole−dipole coupling is at least on the order of magnitude of the homogeneous line width, the dynamics of excitation transfer requires a density matrix approach taking into account coherent excitonic dynamics.[13] Karabunarliev et al.[14] have shown that the features in the electronic spectra of PPV oligomers are primarily due to homogeneous broadening. And because the electronic spectra of PPV and the oligomers are practically equivalent, homogeneous broadening is of greater magnitude than dipole−dipole coupling and the Pauli master equation solution is sufficient. The master equation has also been used in other systems such as multiporphyrin functionalized dendrimers.[28−30]

One chromophore is given the probability of 1 ($P_i = 1$) at $t = 0$, while the rest of the chromophores have zero probability ($P_{i\neq j} = 0$). The probability at i then migrates to the other chromophores as the master equation is integrated through time. Each trimer (OPV3) in the polymer sample was selected in each integration run as the initially excited chromophore. The probability curves of all of the chromphores in the polymer were then used to generate the spectroscopic properties that are discussed in the next section. For comparison, we also calculated the excitation probabilities using tetramers (OPV4) as the initially excited chromophores.

F. Time-Dependent Fluorescence Anisotropy. The time-dependent fluorescence anisotropy, $r(t)$, from a set of chromophores is defined by

$$r(t) = \frac{I_{||}(t) - I_{\perp}(t)}{I_{||}(t) + 2I_{\perp}(t)} \tag{8}$$

where $I_{||}(t)$ is the intensity of the fluorescence signal parallel to the incident polarized radiation and $I_{\perp}(t)$ is the intensity of the signal perpendicular to the incident polarized radiation. In a system in which all of the chromophores remain parallel to each other and to the incident beam, as in a system of chromophores embedded in a crystal, most of the fluorescence signal would

be parallel to the incident signal. Consequently, there will be no loss of anisotropy, and $r(t)$ would remain relatively flat. However if excitation transfer occurs in a system with randomly oriented chromophores, the memory of the orientation of the original signal is lost as the excitation is transferred from one chromophore to another. The intensities of the parallel and perpendicular signals become equal; $r(t)$ approaches zero as anisotropy decays.

As shown in Figure 1, the orientation of the transition dipole moment of an oligomer is not parallel to its long axis but is rotated with a certain angle θ from this direction. Hayes et al.[31] have given a value of 21°; Heeger et al.[32] estimated a much smaller value (<5°), while Spano[33−35] used semiempirical calculations to determine an angle of 8°. In this study, we used an angle of 15°, which is the estimated value that causes the drop in anisotropy at $t = 0$. On the average, this has an effect of further randomizing the orientation of the excitation signals ($I(t)$) and therefore lowering the anisotropy spectrum.

Simulated anisotropy decays of PPV were compared to the experimental results reported by Schwartz and co-workers[9,10] for both bulk MEH−PPV and polymer−mesoporous silica systems. In the single-chain case, a random axis was assigned as the parallel polarization axis. But in the PPV/mesoporous silica case, the parallel polarization axis was defined by the axis of the silica channels.

III. Results and Discussion

A. Time and Length Scales for Energy Transfer in Bulk PPV. Time-dependent red shift has been observed in electroluminescent devices such as PPV. Kersting et al.[24] recorded the highest points of the fluorescence spectra of PPV taken at various times after excitation and showed a fast red shift in the fluorescence spectra of the polymer from 0.1 to 10 ps after excitation and a slow red shift between 10 and 100 ps. No further red shift was detected after 100 ps. However, given the same procedure but using the trimer (OPV3), they observed no red shift, indicating that the mechanism that causes the red shift in the polymer is not present in the trimer. Given that electronic excitation transfer occurs in both samples, it is only in the PPV case that excitation is transferred from one chromophore to another of lower energy because of the presence of an ensemble of oligomer lengths with varying excitation energies. Although the trimer can transfer its electronic excitation to other trimers, the energy of excitation is maintained at the same level. Thus the red shift is observed only in the PPV and not in the OPV3.

Figure 3 shows the excitation probabilities of the oligomers with varying lengths (three to eight phenyl rings) present in the PPV chains. At $t = 0$, we excite the trimers in the system and monitor the evolution of the excitation to oligomers of various lengths. No significant population can be seen for oligomers with more than eight phenyl rings. Because emission at specific times comes from the ensemble of oligomers, the increase in population in longer oligomers with lower emission energies can account for the red shift observed. The time scales are also consistent with experiment because the populations of the longer oligomers do not significantly change after 50 ps. Though the initial decay of the trimer is fast, the decay is much slower after ~20 ps because trimers can act both as donors and acceptors for each other, causing an "equilibrium" between them. This slows down the rates of transfer to other oligomers.

Figure 4 shows the distribution of the distances between the midpoints of the initially excited chromophore (trimers) and the farthest acceptor chromophore that the excitation reaches, assuming at least a 10% population of the acceptor. The average

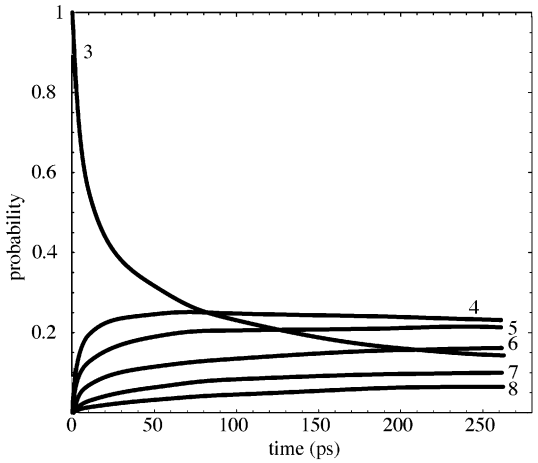

Figure 3. Excitation populations of oligomers with varying lengths (three to eight phenyl rings) with trimers as the initially excited chromophores. The numbers indicate length of the oligomer (number of phenyl rings). Much of the excitation transfer is completed within 50 ps.

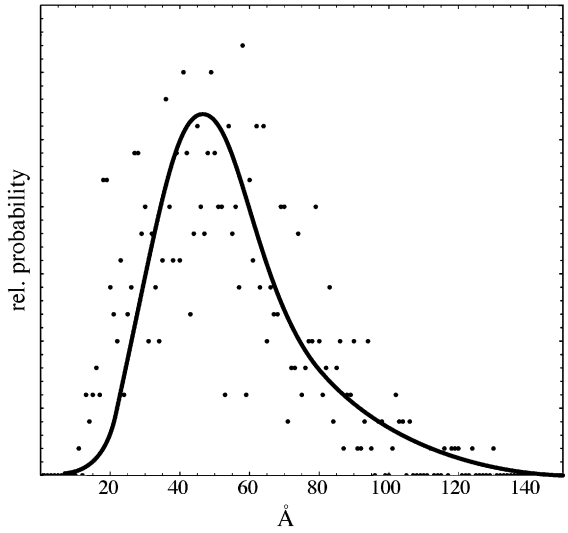

Figure 4. Distribution of distances between an initially excited chromophore and the farthest chromophore that the excitation reaches. The average distance is 51.73 Å. The solid line is the average of the calculated points.

distance, $\langle d \rangle$, is 51.73 Å, the distribution peaking at $d_{max} \approx 47$ Å, although correlation lengths are possible even up to 120 Å. This correlation average is not significantly greater than the calculated Förster distances ($\langle R_0 \rangle = 36.7$ Å). Using the same 10% population criteria, we can estimate that the average number of chromophores involved in the transfer given excitation of one trimer is 3.6 (this includes the initially excited chromophore). Thus on average the excitation finds its energy minima in approximately three jumps within a short average distance of 51.73 Å. For the systems considered, there is a large disparity between the hopping correlation length and the average radius of gyration of 183 Å (for polymers with 1000 Ph−V monomers and 100 cis defects),[7] indicating that the excitation does not travel through most of the polymer but only within a volume close to the initially excited chromophore. For the systems at hand, the global energy minimum coincides with the longest oligomer segment, which can have 10 or more phenyl rings. However, Figure 3 shows that there is very small population for oligomers with eight phenyl rings or more. Contrary to the assumption that excitation always migrates to the lowest-energy state within a density of states, the excitation

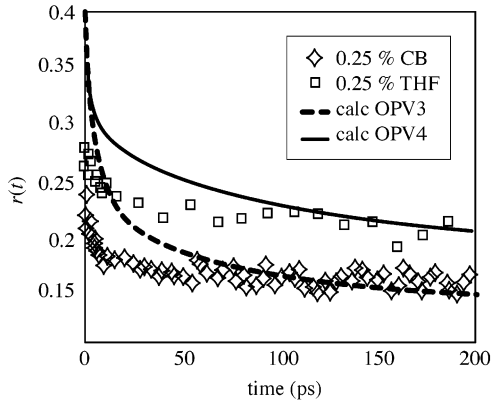

Figure 5. Ultrafast stimulated emission anisotropy of MEH−PPV reported by Schwartz and et al.[9,10] and the calculated anisotropy of PPV using $\epsilon_{max} = 10^4$ M^{-1} cm^{-1}. The two different solution environments are chlorobenzene (◊) and THF (□), both at concentrations of 25% (w/v). The dashed line (calc OPV3) is the calculated anisotropy of PPV with trimers as the initially excited chromophores, while the solid line (calc OPV 4) is for the anisotropy with tetramers as initially excited chromophores.

can be trapped in a nearby local minimum, which can be relatively short conjugated segments with five to eight phenyl rings.

B. Time-Dependent Fluorescence Anisotropy of PPV Chains. Figure 5 shows the experimental stimulated emission anisotropy profiles of single MEH−PPV chains using two different solvents. Schwartz and co-workers[9,10] have argued that aggregation takes place more readily in chlorobenzene (CB) than in tetrahydrofuran (THF). With the chromophores closer to each other, excitation transfer to randomly oriented chromophores occurs more readily in CB than in THF. This accounts for the greater drop and lower equilibrium anisotropy of MEH−PPV in CB as compared to that in a THF solution.

Figure 5 also shows the simulated anisotropy of isolated PPV chains. The dashed line is the anisotropy that we obtain if the trimers are the initially excited chromophores (OPV3 case), while the solid line is for the case in which tetramers are the initially excited chromophores (OPV4 case). The calculated anisotropy generally follows the experimental trend in that as the excitation transfers from one oligomer to another, the memory of the orientation of the initially excited chromophores is lost.

The difference between the OPV3 and OPV4 cases can be rationalized in the following manner. A donor can transfer excitation only if the acceptor is of the same or lower energy of excitation. Trimers transfer their excitation to other trimers, tetramers, and longer oligomers. An initially excited tetramer, however, cannot transfer its excitation to trimers and has fewer candidate acceptor sites therefore lessening the extent of randomization of the orientation of excitation. Consequently, the anisotropy does not relax to the lower and more randomized level as in the OPV3 case.

Although the general trend of the calculated anisotropy follows the experimental data, the plots do not match up perfectly. Förster transfer rates are highly dependent on the Förster distances, which have a contribution of R_0^6 to the rate. An improvement to the point-dipole approximation can have a large effect on the dynamics of the excitation transfer. The same holds true for the calculation of the interchromophore distance ($\propto 1/R^6$). A small discrepancy between the polymer configurations of the model and actual experiment can easily affect the transfer rates. In fact, the MEH−PPV samples in different solvents, which cause different degrees of polymer aggregation

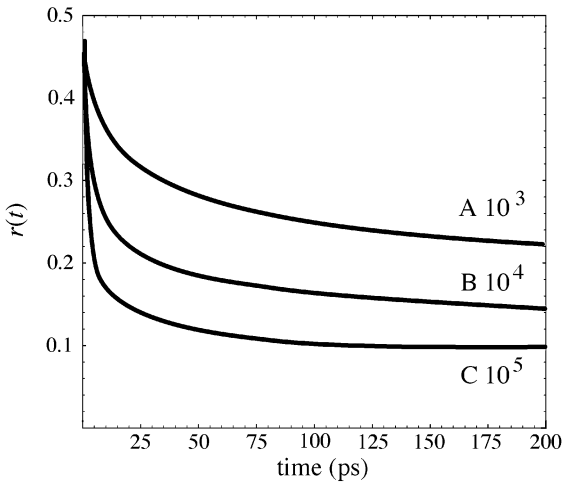

Figure 6. Calculated anisotropy of an ensemble of PPV chains using different extinction coefficients (ϵ_{max}).

TABLE 2: Excitation Transfer Averages Using Various Parameters[a]

run	ϵ_{max} (M^{-1} cm^{-1})	ratio R_0	avg R_0	avg correlation length[b] (Å)	avg number of chromophores[c]
I	10^3	0.6813	24.99	34.08	2.92
II	10^4	1.0	36.68	51.73	3.61
III	10^5	1.478	54.21	73.00	4.29

[a] Trimers were used as the initially excited chromophore. [b] Distance between the initially excited chromophore and the farthest chromophore to which the excitation is transferred. [c] Number of chromophores involved in the excitation transfer process including the initially excited chromophore.

(Figure 5),[6] already show a difference between their transient anisotropy. Other aggregated systems of PPV with a small amount of quencher roughly equivalent to one quencher molecule per PPV chain of 1000 monomers[36,37] exhibited a 95% efficiency in quenching the emission spectrum of the polymer. This can suggest that the excitation transfers throughout the entire polymer to reach the quenching cite. Such a high quenching efficiency will not be reflected in our model because we use a polymer configuration calculation that does not include interatomic forces of attraction that cause the polymer to aggregate.[7] Clearly, systematic improvements in the polymer configuration model and in the use of the point-dipole approximation would easily shift the calculated anisotropy and increase the correlation length, $\langle d \rangle$. However, our goal of this report is to investigate nonradiative excitation transfer as described by Förster theory. And we find our simulations to be in at least qualitative agreement with experimental data. This general agreement is sufficient in supporting the argument that nonradiative energy transfer is fast, occurs in a local area, and finds a local minimum.

C. Sensitivity to Parametrization. Clearly we have made numerous assumptions, particularly in the parametrization of the Förster transfer rates. The simple parameter with the most systematic uncertainty is ϵ_{max}. As mentioned above, this can range over 2 orders of magnitude, and we chose a somewhat moderate value of 10^{-4}. Figure 6 shows the anisotropy plots of PPV using different values of ϵ_{max} and trimers as the initially excited chromophores. The plot for B is the same as the OPV3 plot in Figure 5. Table 2 gives a summary of the results for the change in Förster distance, average Förster distance, average correlation distance, and average number of transfers as a function of ϵ_{max} values. Because the Förster distance is directly proportional to the sixth root of the extinction coefficient (R_0

$\propto \epsilon_{max}^{1/6}$), an increase in ϵ_{max} increases the range of excitation transfer and also increases the average number of jumps in excitation transfer.

Figure 5 shows that using $\epsilon_{max} = 10^4$ is a good estimate because its anisotropy is close to experimental data. However, the averages for the correlation distance and number of transfers for $\epsilon_{max} = 10^5$ are not significantly greater than those for $\epsilon_{max} = 10^4$. In fact, the average correlation distance is still within the radius of gyration of the polymer. The large range of values for the parameters does not alter the conclusion that excitation transfer in PPV does not travel through most of the polymer but only to a relative minimum close to the initially excited chromophore.

D. Intrachain Transfer Model. We also calculated the excitation transfer dynamics neglecting the intrachain transport model proposed in section 2B. There was no observable difference in results whether or not this factor was included. This is because excitation transfer via dipole−dipole coupling is much faster than the proposed intrachain transfer lifetime of 250 ps. Assuming this lifetime is realistic, its effects are therefore not relevant in this study given the time scale difference. However, it is also possible that the actual intrachain transfer rate is much faster than proposed, and this issue of determining this rate deserves greater study.

E. Anisotropy of PPV−Mesoporous Silica Composites. The ultrafast stimulated emission anisotropy of MEH−PPV in mesoporous silica glass, shown in Figure 7a with the data points (circles, squares, and diamonds) and their average (dashed line), shows a fast initial decrease followed by a gradual increase in anisotropy. The gain in anisotropy shows the funneling of excitation from the randomly oriented oligomers outside the channels to the oligomers aligned inside the channels. Figure 2 shows an example of the calculated PPV chains in the mesoporous silica composite. The superimposed circles have radii roughly corresponding to the average correlation length (51.73 Å) for excitation transfer for bulk PPV computed above. Only a few initially excited chromophores can transfer to a nearby chromophore inside the channel (solid circle). Most of the chromophores outside the channels can only reach other chromophores outside the channels (dashed circles). Because the majority of the chains lie outside the radius of the pore, the total anisotropy of an ensemble of random PPV−mesoporous silica configurations (solid line in Figure 7a) would therefore be similar to the anisotropy of the ensemble of polymer chains (Figure 5).

An analysis of the anisotropies of individual samples, however, shows a different picture. Here we use two principal gyration radii to analyze the space taken up by the PPV chains outside the channels. The first corresponds to the radius of gyration for the polymer projected into the *xy*-plane,

$$A = \left[\frac{1}{N}\sum_{i=1}^{N}(\mathbf{r}_i - \mathrm{CTR})^2\right]^{1/2} \tag{9}$$

where $\mathbf{r}_i$ is the position of the carbon atoms using the *x* and *y* coordinates only, CTR is the *xy* coordinates of the center of the three channels, and *N* is the total number of atoms. This value gives us an estimate of how close the chains are to the channels. The second principal radius is

$$B = \left[\frac{1}{N}\sum_{i=1}^{N}(\mathbf{r}_i - c)^2\right]^{1/2} \tag{10}$$

where *c* is the center of mass of the polymers *outside the tube*, and both $\mathbf{r}_i$ and *c* use all three (*xyz*) coordinates. This is the radius of gyration of the polymers outside the channels. These two principal radii can give us an estimate of the proximity of the polymers outside the channels to those inside the channels. Because the average correlation length of excitation transfer, $\langle d \rangle$, is relatively short, a system in which the polymers are compact (low *B* value, or $\langle d \rangle \approx B$) and are close to the channels (low *A* value, or $\langle d \rangle \approx A$) can allow the transfer of excitation from outside to inside the channels.

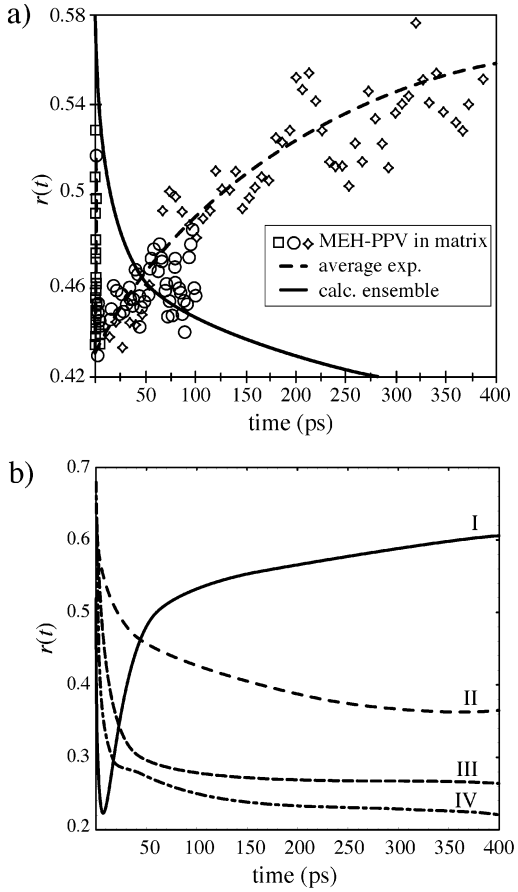

Figure 7. Ultrafast stimulated emission anisotropy (a) of MEH−PPV in mesoporous silica glass with excitation pulse parallel to the pore direction. The points are the experimental data (□, ○, and ◊),[9,10] and the dashed line represents the average of these data. The solid line represents the calculated anisotropy of the ensemble of calculated PPV−mesoporous silica configurations. Panel b shows the calculated anisotropy of the four samples of the calculated PPV−mesoporous silica configurations. The anisotropy of the sample with the lower *A* and *B* parameters (sample I) follows the trend found in experiment.

TABLE 3: *A* and *B* Parameters of Four Samples of Calculated PPV−Mesoporous Silica Configurations

sample	*A* (Å)	*B* (Å)
I	62.27	64.35
II	57.89	76.49
III	70.37	73.53
IV	79.71	72.66

Figure 7b shows the anisotropies of four PPV−mesoporous silica samples with varying *A* and *B* values listed in Table 3. A graphical representation of their relative sizes is shown in Figure 8. The anisotropies of samples II, III, and IV are similar to bulk anisotropy. In these cases, at least one parameter has a large value, indicating that most of the chains outside the channels are not close enough to the channels to promote energy transfer

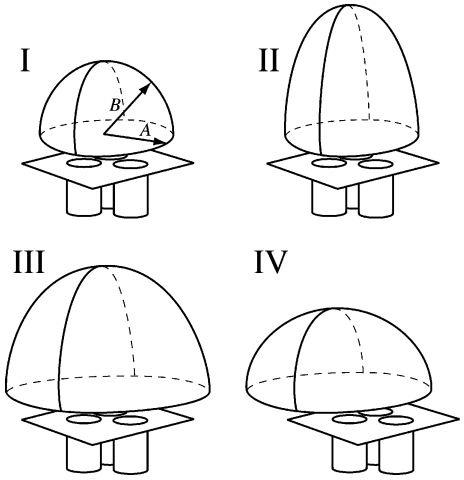

Figure 8. Density of polymer chains outside the mesoporous silica channels. Only sample I has low *A* and *B* values, having outside polymers densely packed close to the channels, thus making the excitation transfer to polymers in the channels possible. The other samples have at least one *A* or *B* value that is large, and the polymers outside are too far from the channels to allow an efficient excitation transfer to the polymers inside.

into these channels. Although the polymers in sample II occupy a small space in the *xy* plane, it spreads upward in the *z*-axis ($A < \langle d \rangle$, $B > \langle d \rangle$). The polymers in sample III spread out in all directions (A and $B > \langle d \rangle$). The polymers in sample IV may not spread as much as seen in samples II or III, but they spread in one direction away from the channels.

The anisotropy of sample I (Figure 7b) has a similar trend to the experimental anisotropy (Figure 7a). After an initial decrease in anisotropy, there is a net gain in anisotropy. Because the polymers outside the channels are compact and close to the center, there is a greater probability that the initially excited chromophores outside the channels would be close enough to facilitate excitation transfer to those in the channels and thus produce a net rise in anisotropy.

The anisotropy of sample I is not of the same scale as the one obtained from experiment (dashed line, Figure 7a). One way to "fit the theory to experiment" is to weight our sample by a 70/30 mix of the anisotropies of samples I and II. One interpretation of this is that the physical system tends to be more aggregated on average than our simulated configurations, which do not include Lennard-Jones-type interactions, and we are simply reweighting our statistical sample toward the true distribution. However, our goal is not to replicate the experimental data exactly but rather to mete out the essential characteristics in excitation transfer to a target site. In the case of the PPV−mesoporous silica system, energy transfer to the chains in the channels is efficient if the polymers outside are compact and close to the polymers in the channels.

IV. Conclusions

Luminescent polymers such as PPV are easy candidates for nonradiative excitation transfer as described by Förster. The set of short and medium length Ph−V oligomers, which act as the chromophores in the chain, have homogeneously broadened spectra, which indicates the dense system of vibrational states assumed in the incoherent coupling between two dipoles of which the transfer rates are described by Förster theory. Calculation of the excitation transfer dynamics confirms the red shift in the emission spectra and loss of anisotropy observed in MEH−PPV. These calculated phenomena were also shown to be very sensitive to spatial parameters. Although a more precise set of parameters and configuration models could replicate experimental data more exactly, the parameters we have used were sufficient to give an insight on the nature of nonradiative excitation transfer.

We have confirmed that Förster transfer is a fast process. We have also shown that the average correlation length of the transfer is fairly small, not significantly larger than the Förster distance, and that on the average only a few chromophores are actually involved in the transfer process for every initially excited chromophore. The excitation does not travel throughout the entire polymer to find the global minimum. Instead, within a short period of time and distance, it easily gets trapped in a local minimum because the global minimum may be out of the Förster transfer range. Assuming that Förster transfer is the only major interchromophore excitation transfer mechanism within the first few picoseconds, the radiative transition to the ground state originates from the relative minimum found in the local area of the initially excited chromophore. This is not consistent with the random walk down the density of states, which assumes the transfer of population from the high-energy short oligomers to the lowest-energy states within the total density of states.

The short correlation distance of excitation transfer also has consequences in the design of energy funneling devices. To achieve a more efficient MEH−PPV−mesoporous silica device, the polymers outside the channels have to be made more compact and clumped close to the targeted system of transfer. One way to achieve this is to use a solvent that promotes aggregation of the polymer chains.

The fast transfer time of <50 ps means that excitation transfers to a local minimum before molecular motions significantly change the configuration of the system. This validates the assumption of using a static polymer configuration to calculate the dynamics of the transfer. This also has consequences in future studies of other forms of energy transfer such as charge transfer or exciton migration. Because these are slower than Förster transfer, one should assume the local minima as the starting point of these these phenomena. Even though the initial excitation energies used are for the high-energy short oligomers, the actual starting point of these other phenomena are the local minima composed of medium to long oligomers.

Acknowledgment. We are grateful to Prof. Benjamin Schwartz for insightful discussions. Funding for this work was provided by the National Science Foundation (Grant CHE-9984416) and the Robert A. Welch Foundation (Grant E-1337).

References and Notes

(1) Pope, M.; Swenberg, C. E. *Electronic Processes in Organic Crystals and Polymers*, 2nd ed.; Oxford Science Publications: New York, 1999.
(2) Yu, J.; Hu, D.; Barbara, P. F. *Science* **2000**, *298*, 1327.
(3) Hu, D.; Yu, J.; Barbara, P. F. *J. Am. Chem. Soc*. **1999**, *121*, 6936.
(4) Vanden Bout, D. A.; Yip, W.-T.; Hu, D.; Fu, D.-K.; Swager, T. M.; Barbara, P. F. *Science* **1997**, *277*, 1074.
(5) Nguyen, T.-Q.; Doan, V.; Schwartz, B. J. *J. Chem. Phys*. **1999**, *110*, 4068.
(6) Nguyen, T.-Q.; Martini, I. B.; Liu, J.; Schwartz, B. J. *J. Phys. Chem. B* **2000**, *104*, 237.
(7) Claudio, G. C.; Bittner, E. R. *J. Chem. Phys*. **2001**, *115*, 9585.
(8) Brédas, J.-L.; Street, G.; Themmans, B.; Andre, J. *J. Chem. Phys*. **1985**, *83*, 1323.
(9) Nguyen, T.-Q.; Wu, J.; Doan, V.; Schwartz, B. J.; Tolbert, S. H. *Science* **2000**, 288, 652.
(10) Schwartz, B. J.; Nquyen, T.-Q.; Wu, J.; Tolbert, S. H. *Synth. Met*. **2001**, 116, 35.
(11) Claudio, G. C.; Bittner, E. R. *Chem. Phys*. **2002**, 276, 81.
(12) Förster, T. *Modern Quantum Chemistry, Part 3*: *Action of Light and Organic Molecules*; Academic Press: New York, 1965; Chapter 3.
(13) May, V.; Kühn, O. *Charge and Energy Transfer in Molecular Systems*; Wiley-VCH: Berlin, 2000.

(14) Karaburnarliev, S.; Baumgarten, M.; Bittner, E. R.; Müllen, K. *J. Chem. Phys.* **2000**, *113*, 11372.
(15) Beljonne, D.; Pourtios, G.; Silva, C.; Hennebicq, E.; Herz, L. M.; Friend, R. H.; Scholes, G. D.; Setayesh, S.; Müllen, K.; Brédas, J.-L. *Proc. Natl. Acad. Sci. U.S.A.* **2002**, *99*, 10982.
(16) Claudio, G. C.; Bittner, E. R.; Beljonne, D.; Hennebicq, E., manuscript in preparation, 2003.
(17) Agranovich, V. M.; Maradudin, A. A. *Electronic Excitation Energy Transfer in Condensed Matter*; North-Holland Publishing Company: New York, 1982.
(18) Karaburnarliev, S.; Baumgarten, M.; Müllen, K. *J. Phys. Chem A* **2000**, *104*, 8236.
(19) Greenham, N. C.; Samuel, I. D. W.; Hayes, G. R.; Phillips, R. T.; Kessener, Y. A. R. R.; Moratti, S. C.; Holmes, A. B.; Friend, R. H. *Chem. Phys. Lett.* **1995**, *241*, 89.
(20) Harris, D. C.; Bertolucci, M. D. *Symmetry and Spectroscopy*; Dover Publications: New York, 1989.
(21) Cornil, J.; Beljonne, D.; Shuai, Z.; Hagler, T. W.; Campbell, I. H.; Bradley, D. D. C.; Brédas, J.-L.; Spangler, C. W.; Müllen, K. *Chem. Phys. Lett.* **1995**, *247*, 425.
(22) Cornil, J.; Beljonne, D.; Heller, C. M.; Campbell, I. H.; Laurich, B.; Smith, D. L.; Bradley, D. D. C.; Müllen, K.; Brédas, J.-L. *Chem. Phys. Lett.* **1997**, *278*, 139.
(23) Grozema, F.; van Duijnen, P. T.; Berlin, Y. A.; Ratner, M. A.; Siebbeles, L. D. A. *J. Phys. Chem. B* **2002**, *106*, 7791.
(24) Kersting, R.; Lemmer, U.; Mahrt, H.; Leo, K.; Bässler, H.; Göbel, E. O. *Phys. Rev. Lett.* **1993**, *70*, 3820.
(25) Rauscher, U.; Bässler, H.; Bradley, D.; Hennecke, M. *Phys. Rev. B* **1990**, *42*, 9830.
(26) Kohler, B. E.; Samuel, I. D. W. *J. Chem. Phys.* **1995**, *103*, 6248.
(27) Kohler, B. E.; Woehl, J. C. *J. Chem. Phys.* **1995**, *103*, 6253.
(28) Heřman, P. Barvík, I. *J. Phys. Chem. B* **1999**, *103*, 10892.
(29) Ghiggino, K. P.; Yeow, E. K. L.; Haines, D. J.; Scholes, G. D.; Smith, T. A. *J. Photochem. Photobiol., A: Chem.* **1996**, *102*, 81.
(30) Yeow, E. K. L.; Ghiggino, K. P.; Reek, J. N. H.; Crossley, M. J.; Bosman, A. W.; Schenning, P. H. J.; Meijer, E. W. *J. Phys. Chem. B* **2000**, *104*, 2596.
(31) Hayes, G.; Samuel, I.; Philips, R. *Phys. Rev. B* **1997**, *56*, 3838.
(32) Hagler, T.; Pakbaz, K.; Heeger, A. *Phys. Rev. B* **1994**, *49*, 10968.
(33) Spano, F. C.; Siddiqui, S. *Chem. Phys. Lett.* **1999**, *314*, 481.
(34) Spano, F. C. *Chem. Phys. Lett.* **2000**, *331*, 7.
(35) Spano, F. C. *J. Chem. Phys.* **2001**, *114*, 5376.
(36) Stork, M.; Gaylord, B. S.; Heeger, A. J.; Bazan, G. C. *Adv. Mater.* **2002**, *14*, 361.
(37) Chen, L.; McBranch, D. W.; Wang, H.-L.; Helgeson, R.; Wudl, F.; Whitten, D. G. *Proc. Natl. Acad. Sci. U.S.A.* **1999**, *96*, 12287.